ISSN 1674-1056
http://cpb.iphy.ac.cn
http://iopscience.iop.org/cpb
中国物理 B
Chinese Physics
中国物理 Chinese Physics B

Optical state selection process with optical pumping in a cesium atomic fountain clock

Lei Han(韩蕾), Fang Fang(房芳), Wei-Liang Chen(陈伟亮), Kun Liu(刘昆), Ya-Ni Zuo(左娅妮), Fa-Song Zheng(郑发松), Shao-Yang Dai(戴少阳), and Tian-Chu Li(李天初)

Citation: Chin. Phys. B, 2021, 30 (**8**): 080602. DOI: 10.1088/1674-1056/ac0698
Journal homepage: http://cpb.iphy.ac.cn; http://iopscience.iop.org/cpb

What follows is a list of articles you may be interested in

Evaluation of second-order Zeeman frequency shift in NTSC-F2

Jun-Ru Shi(施俊如), Xin-Liang Wang(王心亮), Yang Bai(白杨), Fan Yang(杨帆), Yong Guan(管勇), Dan-Dan Liu(刘丹丹), Jun Ruan(阮军), and Shou-Gang Zhang(张首刚)

Chin. Phys. B, 2021, 30 (**7**): 070601. DOI: 10.1088/1674-1056/abe375

Improvement of the short-term stability of atomic fountain clock with state preparation by two-laser optical pumping

Lei Han(韩蕾), Fang Fang(房芳), Wei-Liang Chen(陈伟亮), Kun Liu(刘昆), Shao-Yang Dai(戴少阳), Ya-Ni Zuo(左娅妮), and Tian-Chu Li(李天初)

Chin. Phys. B, 2021, 30 (**5**): 050602. DOI: 10.1088/1674-1056/abe22a

Ramsey-coherent population trapping Cs atomic clock based on lin||lin optical pumping with dispersion detection

Peng-Fei Cheng(程鹏飞), Jian-Wei Zhang(张建伟), Li-Jun Wang(王力军)

Chin. Phys. B, 2019, 28 (**7**): 070601. DOI: 10.1088/1674-1056/28/7/070601

Recent improvements on the atomic fountain clock at SIOM

Du Yuan-Bo, Wei Rong, Dong Ri-Chang, Zou Fan, Wang Yu-Zhu

Chin. Phys. B, 2015, 24 (**7**): 070601. DOI: 10.1088/1674-1056/24/7/070601

Design and test of the microwave cavity in an optically-pumped Rubidium beam frequency standard

Liu Chang, Wang Yan-Hui

Chin. Phys. B, 2015, 24 (**1**): 010602. DOI: 10.1088/1674-1056/24/1/010602

Optical state selection process with optical pumping in a cesium atomic fountain clock*

Lei Han(韩蕾)[1], Fang Fang(房芳)[2,†], Wei-Liang Chen(陈伟亮)[2], Kun Liu(刘昆)[2], Ya-Ni Zuo(左娅妮)[2], Fa-Song Zheng(郑发松)[2], Shao-Yang Dai(戴少阳)[2], and Tian-Chu Li(李天初)[1,2,‡]

[1] *School of Optics and Photonics, Beijing Institute of Technology, Beijing* 100081, *China*

[2] *Key Laboratory of Time and Frequency Standards, National Institute of Metrology (NIM), Beijing* 100029, *China*

(Received 20 February 2021; revised manuscript received 8 April 2021; accepted manuscript online 29 May 2021)

We propose and realize a new optical state selection method on a cesium atomic fountain clock by applying a two-laser 3–3′ optical pumping configuration to spin polarize atoms. The atoms are prepared in $|F=3, m_F=0\rangle$ clock state with optical pumping directly after being launched up, followed by a pushing beam to push away the atoms remaining in the $|F=4\rangle$ state. With a state selection efficiency exceeding 92%, this optical method can substitute the traditional microwave state selection, and helps to develop a more compact physical package. A Ramsey fringe has been achieved with this optical state selection method, and a contrast of 90% is obtained with a full width half maximum of 0.92 Hz. The short-term frequency stability of 6.8×10^{-14} $(\tau/\mathrm{s})^{-1/2}$ is acquired. In addition, the number of detected atoms is increased by a factor of 1.7 with the optical state selection.

Keywords: optical pumping, atomic fountain clock, spin polarization, optical state selection

PACS: 06.30.Ft, 31.15.–p, 32.10.Fn, 32.80.Xx **DOI:** 10.1088/1674-1056/ac0698

1. Introduction

The cesium fountain clocks have operated as primary frequency standards (PFS) to realize the definition of the SI second, which have many significant applications in science and technology, such as time-keeping, high accuracy metrology, and navigation and positioning systems.[1–3] A typical type-B uncertainty now reaches a few parts in 10^{-16} and a type-A uncertainty has achieved 10^{-13}–10^{-14} $(\tau/\mathrm{s})^{-1/2}$, limited by the quantum projection noise or a local oscillator phase noise.[4–15] Generally, about 10^6–10^8 atoms are collected and only about 10% of them contribute to the detection signal.[16–18] Spin-polarized atoms with optical pumping (OP) have been widely applied in atomic and nuclear physics, such as atomic clocks, atomic magnetometers, and hyperpolarized magnetic resonance imaging.[19–23] The optical pumping of several two-laser schemes in a cesium beam has been investigated with rate-equation model in Ref. [24]. In the atomic fountain, a two-laser 4–4′ OP scheme is implemented to increase the atomic signal, allowing an improvement of the fountain clock stability.[16,25] Another two-laser 3–3′ OP scheme has also been applied to a continuous atomic fountain, preparing only more than 50% of the atoms in the $|F=3, m_F=0\rangle$ state, to improve the signal-to-noise ratio (SNR) of the fountain.[21]

In the cesium fountain frequency standards, all the atoms are approximately distributed evenly in the 9 Zeeman sublevels of $|F=4\rangle$ state after being launched. A state selection process to select only atoms in the clock state is essential to obtain a good SNR, reduce the collisional shift, suppress the Rabi and Ramsey pulling cavity effect, and inhibit the Majorana transitions effect.[4–6] With the routine microwave state selection method, atoms in the $|F=4, m_F=0\rangle$ state are transferred to the $|F=3, m_F=0\rangle$ clock state by a microwave pulse in a state selection cavity, and the residual atoms in the $|F=4, m_F\neq0\rangle$ states will be pushed away by a laser pulse, resulting in a approximately 90% loss of atoms.

In this paper, a new optical state selection method to pump atoms directly to the $|F=3, m_F=0\rangle$ state in a Cs fountain clock is realized for the first time. Not only the state selection cavity can be removed for a more compact physical package, but also more atoms will be accumulated in the $|F=3, m_F=0\rangle$ clock state. To obtain a good Ramsey fringe contrast and keep low uncertainties of physically related frequency shift, it is critical to push away the atoms in the non-clock states. After the introduction of experimental setup, theoretical simulation is carried out to estimate the effect of the stray magnetic field and the purity of the OP laser polarization on the state selection efficiency. Furthermore, a state selection efficiency of 92% is obtained in experiment, and the detection signal has increased by 70% while the contrast of the central Ramsey fringe exceeds 90% with a full width half maximum (FWHM) of 0.92 Hz, which demonstrates the promising performance of our method.

*Project supported by the National Natural Science Foundation of China (Grant No. 11873044).

†Corresponding author. E-mail: fangf@nim.ac.cn

‡Corresponding author. E-mail: litch@nim.ac.cn

© 2021 Chinese Physical Society and IOP Publishing Ltd

2. System design and theoretical analysis

2.1. System design

The design and operation of the fountain clock used in our experiment are described elsewhere.[17,26,27] Here, only the essential part related to the optical state selection is introduced. A master laser is locked to the $|F=4\rangle \rightarrow |F'=4\rangle$ transition, and frequency-shifted to $|F=4\rangle \rightarrow |F'=3\rangle$ transition by an AOM as the de-pump light. Another laser is locked to the crossover of $|F=3\rangle \rightarrow |F'=3\rangle$ and $|F=3\rangle \rightarrow |F'=4\rangle$ transitions, and shifted to $|F=3\rangle \rightarrow |F'=3\rangle$ transition for optical pumping. All the lasers are guided from the optical bench to the atomic fountain by polarization-maintaining optical fibres.

As indicated in Fig. 1(a), the region for optical state selection locates 32 mm above the center of the optical molasses (OM) chamber. The optical pumping light and de-pump light are combined through a fiber beam splitter and injected into the same polarization-maintaining fiber, then the combined beam passes through a polarized beam splitter (PBS) with an extinction ratio over 500 for transmitted P polarization to obtain a purely linearly polarized light. A $\lambda/2$ waveplate is used to fine tune the alignment of light's polarization direction and magnetic field direction. A pair of approximate Helmholtz coils, whose center coincides with the center of the optical state selection zone, is applied to generate a uniform magnetic field along the z-axis during the optical state selection process. To reduce the loss of atoms due to the radiation pressure during the OP process, a reflector M2 is introduced to form a standing-wave field for OP lights.

To substitute the microwave state selection with optical state selection, the temporal evolution of atomic distribution is analyzed and the relevant time sequence is adjusted. Atoms will distribute evenly in the $|F=4\rangle$ state after being launched. As depicted in Fig. 1(c), the coils for optical state selection (pink pulse) are turned on right after the atoms being launched (black pulse). Then the atoms will be pumped to the $|F=3\rangle$ state first except for those in the $|F=4,\ m_F=\pm4\rangle$ states (see Fig. 1(b)) by the de-pump light (blue pulse) when passing through the OP region during their ascending trajectory. Since the $|F=3,\ m_F=0\rangle \rightarrow |F'=3,\ m_{F'}=0\rangle$ transition is forbidden according to the angular-momentum selection rules as indicated in Fig. 1(b), the OP and de-pump lights lead to the atom-population accumulation in the $|F=3, m_F=0\rangle$ state. To minimize the atom population in the $|F=3,\ m_F\neq0\rangle$ states, the de-pump light should be turned off earlier than the OP light as depicted in Fig. 1(c). Thus, only atoms in $|F=3,\ m_F\neq0\rangle$ and $|F=4\rangle$ states are left. Then the atoms in the $|F=4\rangle$ state will be removed when they pass through the detection zone corresponding to the first green pulse in Fig. 1(c), similar to a routine fountain operation. Thereby, the 3–3′ OP method accomplishes the optical state selection and optical pumping in one step, which is an essential advantage over the 4–4′ OP method. Although more atoms will be prepared in the $|F=4,\ m_F=0\rangle$ state with the 4–4′ OP method, a pulsed microwave to pump atoms to the $|F=3,\ m_F=0\rangle$ state is indispensable for the state selection. Whereas in the 3–3′ OP method, the optical state selection can substitute the microwave state selection, thus the microwave selection cavity is not necessary. This is beneficial not only to simplify the physical package, but also to avoid the resonant interference between the interrogation microwave source and state selection microwave source.

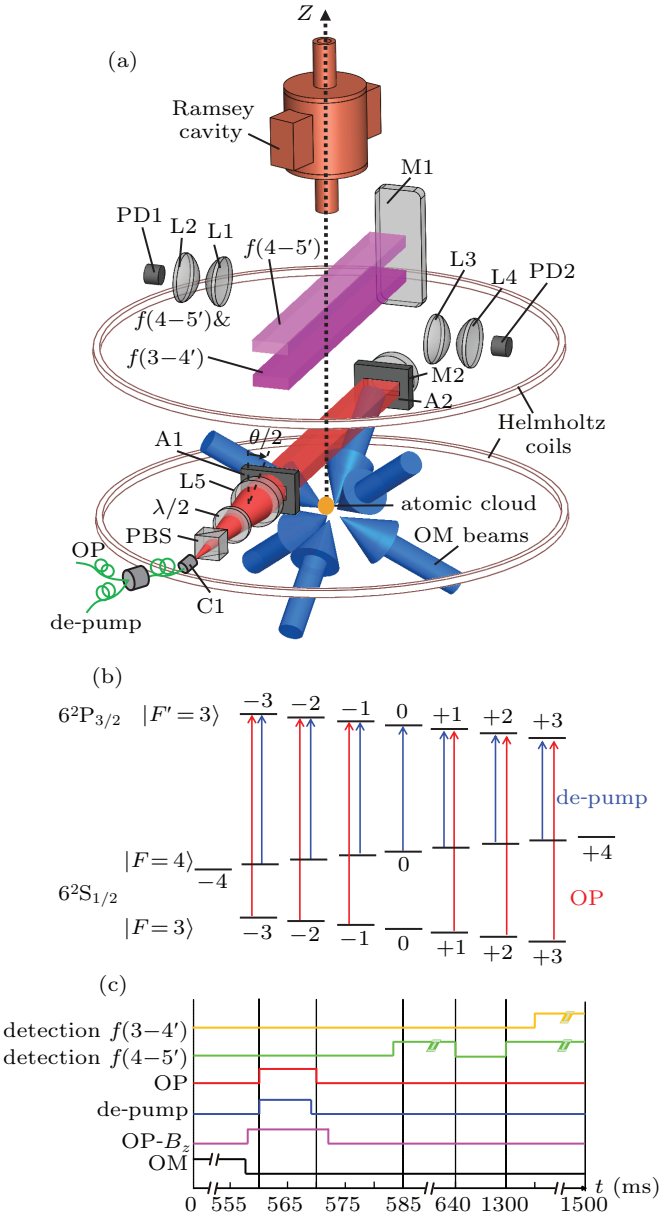


Fig. 1. (a) Experimental setup. A: aperture; L: lens; M: mirrors; PD: photoelectric detector; C: fibre coupler; Three pairs of orthogonal cooling lasers (blue) counter-propagate in the OM region and intersect at the same center on the z-axis. The OP beams are 32 mm above the OM center. (b) Energy level diagram of cesium D_2 transition for optical state selection configuration. The forbidden transition of $|F=3,\ m_F=0\rangle \rightarrow |F'=3,\ m_{F'}=0\rangle$ is used to accumulate atoms in the $|F=3,\ m_F=0\rangle$ state. The energy gaps are not in scale. (c) Relevant time sequence diagram of the experiment. The time sequences of atoms collecting with magneto optical trap (MOT), atoms launching, post cooling, and Ramsey pulse are not shown in the figure.

Afterwards, only the atoms in the $|F=3\rangle$ states pass through the same interrogation microwave cavity twice during the ascending and descending trajectory to experience a Ramsey interrogation and the clock transition $|F=3,\ m_F=0\rangle \rightarrow |F=4,\ m_F=0\rangle$ is excited. Finally, the atoms fall into the detection region, passing through the first transverse standing-wave beam with its frequency on resonance with $|F=4\rangle \rightarrow |F'=5\rangle$ transition and the atoms in the $|F=4\rangle$ state will be excited, as indicated as the second green pulse in Fig. 1(c). Its fluorescent signal will be detected with integrating the TOF signal, which is proportional to the number of atoms N_4 in the $|F=4\rangle$ state. Then the atoms in the $|F=4\rangle$ state are pushed away by a travelling-wave in the lower part of the upper detection beam, and only the atoms in the $|F=3\rangle$ state keep falling. Subsequently, the combined laser beams, in which one's frequency is tuned to $|F=3\rangle \rightarrow |F'=4\rangle$ transition (the orange pulse in Fig. 1(c)) and the other is tuned to $|F=4\rangle \rightarrow |F'=5\rangle$ transition (the second green pulse in Fig. 1(c)), are applied to pump the remaining atoms in $|F=3\rangle$ state to $|F=4\rangle$ state first and the fluorescent signal is detected accordingly, which is proportional to the number of atoms N_3 in the $|F=3\rangle$ state. The transition probability P defined as $P=N_4/N_3+N_4$ can be derived, which is used as the input signal for the microwave-frequency locking servo loop.[4]

2.2. Theoretical simulation

Different from the 4–4′ OP where a high OP efficiency $N_{4,0}/(N_3+N_4)$ is expected, in 3–3′ OP method it is critical to keep a high state selection efficiency of $N_{3,0}/N_3$ to ensure a good contrast of Ramsey fringe and a low related frequency uncertainty, where $N_{3,0}$ and N_3 denote the atom populations in the $|F=3,\ m_F=0\rangle$ state and in all $|F=3,m_F\rangle$ Zeeman sublevels, respectively. As described in the previous section, the OP laser is supposed to be a purely π-polarized light, otherwise, the $|F=3,m_F=0\rangle$ state will not be a dark state. Therefore, the purity of the OP laser polarization and the coincidence between the magnetic field direction and linear polarization direction of the laser beams are inevitably limiting factors to the optical state selection efficiency. To simulate the constraints of these effects, the temporal evolution of atom populations on each sublevel is calculated with the rate-equation model,[24] under the conditions of weak laser intensity, finite laser linewidth, and negligible atomic linewidth.

The optical state selection efficiency and the average number of photons scattered per atom $n_{\rm phon}$ within the OP's duration are plotted in Fig. 2 for different parameters. In Figs. 2(a) and 2(b), the optical state selection efficiency increases to over 90% during a short OP pulse with low OP laser intensities, indicating that a higher laser intensity leads to a more rapid growth of the selection efficiency, while keeping the number of scattered photons small. The OP laser intensity on the order of tens of $\mu W\cdot cm^{-2}$ is adequate for the experiment.

The optical state selection efficiency depends on the coincidence between the linear polarization direction of the OP beam and the magnetic field direction, with θ denoting their tilt angle, as illustrated in Figs. 2(c) and 2(d). The intensities of OP and de-pump laser are 20 $\mu W\cdot cm^{-2}$ and 100 $\mu W\cdot cm^{-2}$, respectively. With a tilt angle θ, namely, some σ-polarized component, the optical state selection efficiency drops compared to the result under $\theta=0$ condition. Also, it increases more slowly as the OP's duration lengthens, and the number of scattered photons also increases rapidly.

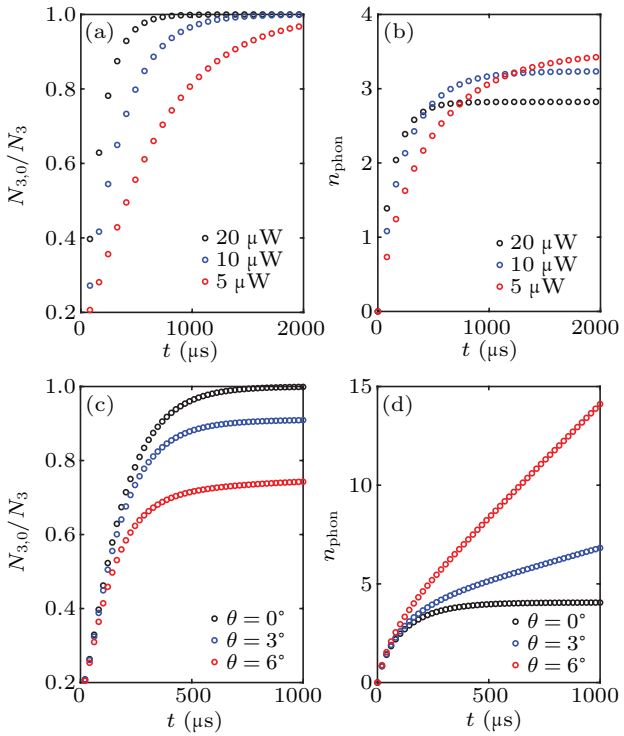


Fig. 2. Theoretical simulations of temporal dynamics of optical state selection based on 3–3′ OP method with different parameters. Panels (a) and (b) show the optical state selection efficiencies and the average number of photons scattered per atom as a function of OP's duration, respectively for different laser intensities. Black, blue, and red markers correspond to the OP laser intensity of 20 $\mu W\cdot cm^{-2}$, 10 $\mu W\cdot cm^{-2}$, and 5 $\mu W\cdot cm^{-2}$, respectively, with the de-pump laser intensities of 100 $\mu W\cdot cm^{-2}$. Panels (c) and (d) indicate the effect caused by the nonideal polarization of the laser beams, and θ represents the tilt angle between the linear polarization direction of the OP beam and the magnetic field direction.

The 3–3′ OP configuration shows prominent advantages of increasing optical state selection efficiency and attenuating heating effect under the conditions of weak laser intensity and short OP pulse duration, which is promising in atomic fountain clocks.

3. Results and discussion

Based on the above mentioned theoretical calculations, this optical state selection process is carried out by replacing the microwave state selection on the NIM6 cesium atomic

fountain clock. The results are discussed in the following.

Figure 3 shows the dependences of the optical state selection efficiency on the laser intensity and the frequency detuning from resonance. In our experiment, the OP pulse's duration is about 3 ms, limited by the beam height of OP and atomic launching velocity. The optical state selection efficiency gradually increases up to 90% and tends to be stable with the increase of the OP laser intensity as shown in Fig. 3(a). It suggests that a higher laser intensity is required to maintain a high optical state selection efficiency when the OP laser frequency has a certain detuning. The adequate OP laser intensity of 3–3′ OP in this experiment is tens of $\mu W{\cdot}cm^{-2}$.

The gain of the detected atom numbers (by integrating the TOF signal) with optical state selection relative to the microwave state selection is measured and shown in Fig. 3(b). At a weak laser intensity, the gain of the detection signal increases with the OP intensity. On further increasing the intensity of OP, the gain tends to be saturated and then decreases due to the heating effect of atoms. The saturation point of each curve in Fig. 3(b) agrees with the results in Fig. 3(a). Comparing the downtrend of three different detuning curves, we can deduce that a near-resonant laser gives rise to more serious heating as the OP intensity increases, which is characterized by the gain reduction. The tilt angle is about 2.5° due to the 0.2%-impurity of laser polarization in our experiment, corresponding to a theoretical average number of 6 for photons scattered per atom.

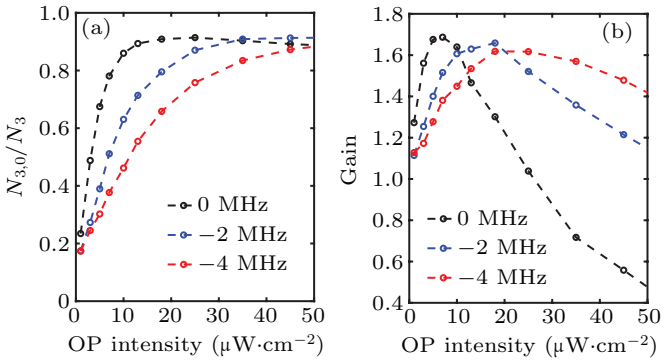


Fig. 3. (a) The measured state selection efficiency as a function of OP light intensity at different frequency detunings. (b) The effect of OP light intensity and frequency detuning on the gain of detection signal. The black, blue, and red circles denote the detuning of 0 MHz, −2 MHz, and −4 MHz, respectively. The dashed lines link the data points for clarity.

Moreover, the dependence of the optical state selection efficiency on the tilt angle θ, which reflects the polarization purity of the OP laser, is measured and shown in Fig. 4(a). The experimental results agree very well with the theoretical calculations. Besides the aforementioned residual magnetic field on the horizontal plane and the OP laser polarization impurity, the optical state selection efficiency is also affected by the reabsorption of unpolarized light emitted from the atomic cloud called the shadow effect.[16] A larger atomic cloud will require a larger uniform magnetic field, which also restricts the gain of the detection signal. This effect is checked by varying the total number of atoms with different MOT loading time, as the gain being plotted in Fig. 4(b) for the relative atomic density.

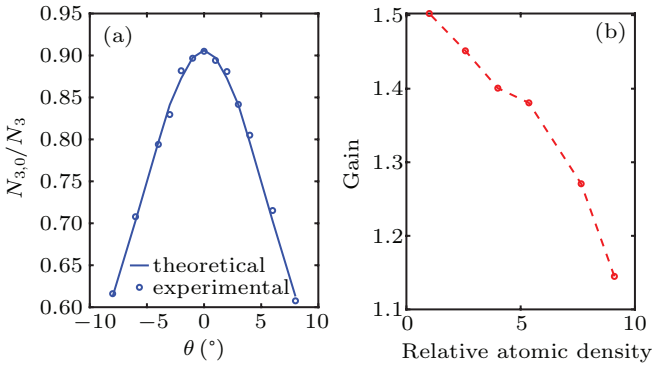


Fig. 4. (a) The state selection efficiency as a function of the tilt angle θ. The blue circles denote the experimental data points while the solid line represents the theoretical values. (b) The effect of atomic density on the gain of the detection signal. The red circles represent the measured data points, linked by dashed lines for clarity.

With the optical state selection method by 3–3′ OP configuration, the number of detected atoms is 1.7 times of that obtained with microwave state selection (shown in Fig. 3(b)), and the atom population in $|F=3, m_F=\rangle$ state accounts for more than 90% of the atom population in $|F=3\rangle$ state, implying an optical state selection efficiency exceeding 90% (shown in Fig. 3(a)). Although the results have shown a high optical state selection efficiency and a larger detection signal, the gain of the detected atom numbers is still lower than expected. One dominant reason is that the atoms in $|F=4, m_F=\pm4\rangle$ states are dark states for de-pumping, which accounts for about 22% of the total atom number. Another reason is that the de-pump laser is combined with the OP laser spatially, whose polarization cannot be optimized independently.

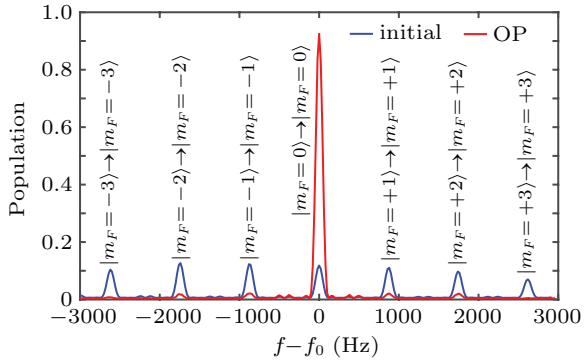


Fig. 5. The atom populations on m_F sublevels with (red line) and without (blue line) optical state selection.

A Rabi-type microwave spectroscopy is applied to excite the $|F=4\rangle \rightarrow |F=3, \Delta m_F=0\rangle$ transition. The peak heights represent the initial atom populations of $|m_F\rangle$ states as shown in Fig. 5, whereas the $|m_F=\pm4\rangle$ states cannot be measured. Similarly, the atom-population distribution among $|F=3\rangle$ states after optical state selection is determined. The optical state selection efficiency increases up to 92% with

good symmetry of the population distribution. The ratios of $(N_{3,+m_F} - N_{3,-m_F})/N_3$ are 0%, 0.1%, and 0.3% for m_F from 1 to 3, respectively.

To verify that the optical state selection can completely replace the microwave state selection in the operation of an atomic fountain clock, the Ramsey fringe of the $|F = 3, m_F = 0\rangle \rightarrow |F = 4, m_F = 0\rangle$ transition is obtained as shown in Fig. 6(a) with the inset representing the central fringe. The FWHM of the central fringe is 0.92 Hz and the contrast is 90%. And the short-term frequency stability of the fountain clock with the optical state selection method is derived as $\sigma_y(\tau) = 6.8 \times 10^{-14}\tau^{-1/2}$, as shown in Fig. 6(b).

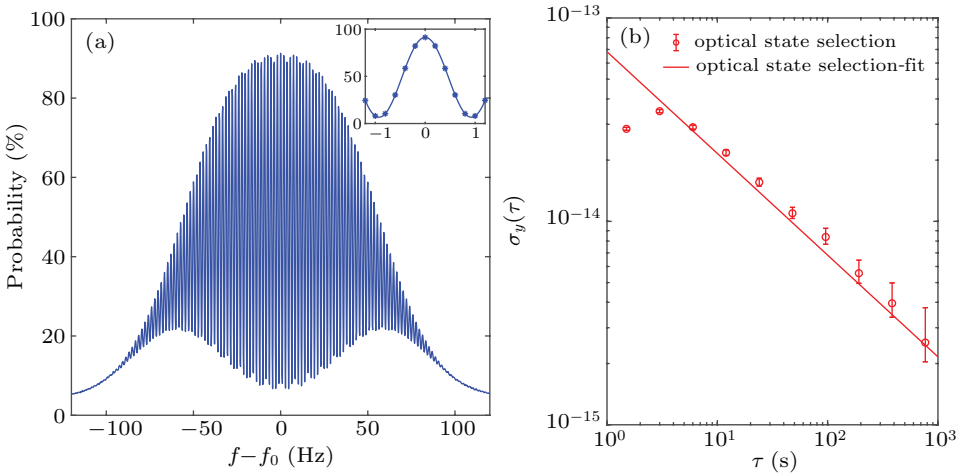


Fig. 6. The results of atomic fountain clock operation with optical state selection. (a) Ramsey fringe of the Cs fountain clock NIM6 (the transition probability as a function of the frequency detuning) of the $|F = 3, m_F = 0\rangle \rightarrow |F = 4, m_F = 0\rangle$ transition with a frequency scanning step of 0.2 Hz without averaging. The inset shows the central Ramsey fringe. (b) The short-term frequency stability of Cs fountain clock NIM6 with optical state selection expressed as an Allan standard deviation with a cycle time of 1.5 s.

4. Conclusion and future works

Considering the large size of a microwave cavity, the overall atomic fountain clock physical package is unfavorable for a compact and portable fountain clock. Furthermore, the frequency of the microwave state selection source is close to that of the interrogation microwave source, which will result in noise coupling.

A new optical state selection method with a 3–3′ optical pumping configuration is presented to substitute the microwave state selection in a Cs fountain clock. The effects of the stray magnetic field and the impurity of the OP light polarization on the optical state selection efficiency are theoretically analyzed. Furthermore, the optical state selection is implemented experimentally on the NIM6 Cs fountain clock instead of microwave state selection cavity, and a state selection efficiency of 92% is achieved while a good contrast of Ramsey fringe and a short-term frequency stability of 6.8×10^{-14} $(\tau/\mathrm{s})^{-1/2}$ are obtained. In a Rb fountain clock, it will show a better performance due to fewer Zeeman sublevels. Moreover, the gain of the detected atom number is determined to be 1.7, which is expected to be further improved by separating the OP and de-pump laser beams spatially for optimizing their polarizations independently.

References

[1] Bauch A, Weyers S, Piester D, Stalimuniene E and Yang W 2012 *Metrologia* **49** 180

[2] Rosenband T, Hume D B, Schmidt P O, Chou C W, Brusch A, Lorini L, Oskay W H, Drullinger R E, Fortier T M, Stalnaker J E, Diddams S A, Swann W C, Newbury N R, Itano W M, Wineland D J and Bergquist J C 2008 *Science* **319** 1808

[3] Wolf P, Chapelet F, Bize S and Clairon A 2006 *Phys. Rev. Lett.* **96** 060801

[4] Wynands R and Weyers S 2005 *Metrologia* **42** S64

[5] Fang F, Li M S, Lin P W, Chen W L, Liu N F, Lin Y G, Wang P, Liu K, Suo R and Li T C 2015 *Metrologia* **52** 454

[6] Weyers S, Gerginov V, Kazda M, Rahm J, Lipphardt B, Dobrev G and Gibble K 2018 *Metrologia* **55** 789

[7] Szymaniec K, Park S E, Marra G and Chalupczak W 2010 *Metrologia* **47** 363

[8] Vian C, Rosenbusch P, Marion H, Bize S, Cacciapuoti L, Zhang S, Abgrall M, Chambon D, Maksimovic I, Laurent P, Santarelli G, Clairon A, Luiten A, Tobar M and Salomon C 2005 *IEEE Trans. Instrum. Meas.* **54** 833

[9] Guena J, Abgrall M, Rovera D, Laurent P, Chupin B, Lours M, Santarelli G, Rosenbusch P, Tobar M E, Li R X, Gibble K, Clairon A and Bize S 2012 *IEEE Trans. Ultrason. Ferroelectr. Freq. Control* **59** 391

[10] Heavner T P, Jefferts S R, Donley E A, Shirley J H and Parker T E 2005 *Metrologia* **42** 411

[11] Takamizawa A, Yanagimachi S, Tanabe T, Hagimoto K, Hirano I, Watabe K, Ikegami T and Hartnett J G 2015 *IEEE Trans. Instrum. Meas.* **64** 2504

[12] Levi F, Calonico D, Calosso C E, Godone A, Micalizio S and Costanzo G A 2014 *Metrologia* **51** 270

[13] Levi F, Lorini L, Calonico D and Godone A 2004 *IEEE Trans. Ultrason. Ferroelectr. Freq. Control* **51** 1216

[14] Weyers S, Hubner U, Schroder R, Tamm C and Bauch A 2001 *Metrologia* **38** 343

[15] Dai S Y, Zheng F S, Liu K, Chen W L, Lin Y G, Li T C and Fang F 2021 *Chin. Phys. B* **30** 013701

[16] Szymaniec K, Noh H R, Park S E and Takamizawa A 2013 *Appl. Phys. B* **111** 527

[17] Fang F, Chen W L, Liu K, Liu N F, Suo R and Li T C 2015 *Joint Conference of theIEEE International Frequency Control Symposium & the European Frequency and Time Forum*, April 12–16, 2015 Denver, USA, pp. 492–494

[18] Santarelli G, Laurent P, Lemonde P, Clairon A, Mann A G, Chang S, Luiten A N and Salomon C 1999 *Phys. Rev. Lett.* **82** 4619
[19] Happer W 1972 *Rev. Mod. Phys.* **44** 169
[20] Wang Z G, Jiang Q Y, Zhan X, Chen Y D and Luo H 2016 *AIP Advances* **6** 085110
[21] Domenico G D, Devenoges L, Dumas C and Thomann P 2010 *Phys. Rev. A* **82** 053417
[22] Allred J C, Lyman R N, Kornack T W and Romalis M V 2002 *Phys. Rev. Lett.* **89** 130801
[23] Walker T G and Happer W 1997 *Rev. Mod. Phys.* **69** 629
[24] Avila G, Giordano V, Candelier V, Clercq E D, Theobald G and Cerez P 1987 *Phys. Rev. A* **36** 3719
[25] Han L, Fang F, Chen W L, Liu K, Dai S Y, Zuo Y N and Li T C 2021 *Chin. Phys. B* **30** 050602
[26] Fang F, Chen W L, Liu K, Dai S Y, Liu N F, Han L, Zheng F S and Li T C 2019 *Joint Conference of the IEEE International Frequency Control Symposium and the European Frequency and Time Forum*, April 14–18, 2019, Orlando, USA, 8856067
[27] Dai S Y, Fang F, Liu K, Chen W L, Liu N F, Cao S Y and Li T C 2020 *AIP Advances* **10** 065118